Catalysis Letters 17 (1993) 117–126

Identification of Pd^{3+} ions in zeolite L by temperature programmed reduction and electron paramagnetic resonance spectroscopy

Sanjay N. Gandhi, Guan-Dao Lei and Wolfgang M.H. Sachtler [1]

V.N. Ipatieff Laboratory, Center for Catalysis and Surface Science, Northwestern University, Evanston, IL 60208, USA

Received 29 June 1992; accepted 27 October 1992

Pd supported on KL zeolite has been studied by temperature programmed reduction (TPR) and electron paramagnetic resonance (EPR) spectroscopy. It has been found that upon calcination in pure oxygen Pd^{3+} and Pd^{2+} ions are formed; the Pd^{3+} ions are identified by their EPR signal. As Pd^{3+} ions in the cancrinite cages are difficult to reduce, the H_2 consumption in conventional TPR is below the stoichiometric amount.

Keywords: Pd^{3+} in zeolite L; EPR of Pd^{3+}; TPR of Pd/L

1. Introduction

Pt/KL is a non-acidic reforming catalyst displaying a high selectivity for the conversion of *n*-hexane to benzene [1]. Two approaches to explain this high activity and selectivity have tried to attribute the catalytic properties to either the electronic state of the metal [2,3] or to geometric effects due to the linear channels of zeolite L [4–10]. No consensus has been reached on the state of Pt in these catalysts at various stages of catalyst preparation and pretreatment, primarily due to the difficulties involved in the characterization of Pt.

Supported Pt has been found to exist in a variety of oxidation states ranging from Pt^{2+} to Pt^{4+} [7,11–14]. Pt also undergoes autoreduction due to the action of decomposing ammine ligands of the metal precursor. In an oxidizing atmosphere the reduced Pt particles are subsequently partly oxidized, leading to a distribution of oxides and ions of Pt [7,15].

Ostgard et al. [7] performed temperature programmed reduction and found that the TPR profiles of Pt in catalysts prepared by ion-exchange and incipient

---

[1] To whom correspondence should be addressed.

wetness impregnation were markedly different. After calcination, the ion-exchanged catalysts contain PtO particles which are reduced at 11°C, and two forms of Pt^{2+} ions that are reduced at 80 and 150°C, respectively. On the other hand, catalysts prepared by incipient wetness contain predominantly Pt^{4+} ions. Zeolite supported Pt cannot be characterized by X-ray photoelectron spectroscopy since the Pt signal overlaps the major signal for the Al which is present in the zeolite.

To avoid these difficulties, we have prepared and characterized Pd catalysts supported on KL assuming that this will provide some understanding of the chemistry of Pd, and indirectly also of Pt, in zeolite L. Previous results revealed many close similarities between Pt and Pd supported on HY and NaY with respect to metal particle formation and location [16,17]. Pd does not autoreduce in HY or NaY [16,17], and Pd ions are predominantly found to be in the Pd^{2+} oxidation state. However, some recent studies have identified Pd^{1+}, Pd^{3+} and Pd^{4+} under various conditions in zeolites [18–21].

In the present paper we report on Pd/KL catalysts prepared by ion-exchange and characterized by temperature programmed reduction and electron paramagnetic resonance spectroscopy to determine the oxidation state and location of Pd in L zeolite.

2. Experimental

2.1. CATALYST PREPARATION AND PRETREATMENT

3 wt% Pd/KL catalysts were prepared. KL support was obtained from Tosoh Corp (HSZ-500 KOA). Pd was introduced into these supports by ion-exchange. A solution of $Pd(NH_3)_4(NO_3)_2$ was added dropwise to a continuously stirred slurry of the support in doubly deionized water (200 ml/g). The ion-exchange was carried out for a period of 36 h. The slurry was filtered, washed with doubly deionized water and air dried for 24 h. Prior to the TPR studies, the catalyst was calcined in a flow of UHP O_2 with the temperature being ramped from room temperature to the desired calcination temperature at 0.5°C/min and held at this temperature for 2 h. After this the gas flow was changed to UHP Ar (200 ml min^{-1} g^{-1}) and held at the calcination temperature for 20 min, before cooling to room temperature.

2.2. TEMPERATURE PROGRAMMED REDUCTION

The apparatus and procedure for the temperature programmed reduction experiments were described in previous papers [22,23]. After calcination up to the desired temperature the catalyst is cooled in UHP Ar to -78°C using a dry ice/acetone bath. The gas flow is then changed to a 5% H_2 in Ar stream. The temperature of the catalyst bed is then ramped at 8°C/min from −78 to 300°C and the sample was held at the reduction temperature for 10 min. During this time the hydrogen consumption is continuously monitored by a thermal conductivity detector (TCD) cell.

2.3. TEMPERATURE PROGRAMMED REDUCTION-MASS SPECTROMETRY

TPR-MS measurements were carried out in the same way as described above, except that the gases from the outlet of the reactor are analyzed using an on-line Dycor mass spectrometer.

2.4. TPR-REOXIDATION

These experiments are done primarily to ensure the accuracy of the measurements using the TCD cell and to identify the species that is present at the end of the calcination and reduction steps. After the TPR the temperature of the catalyst bed is lowered to 100°C. At this point the gas flow is changed to 150 ml/min of UHP O_2. The catalyst is then treated with UHP O_2 for 1 h at 100°C, after which the gas flow is switched to UHP Ar and cooled to −78°C. After this a second TPR is carried out.

2.5. ELECTRON PARAMAGNETIC RESONANCE

EPR spectra for different samples were recorded at 77 K and at room temperature with a modified Varian E-4 spectrometer. The reactor was connected to a small quartz tube. The samples were prepared and then collected in a quartz tube. After evacuation the quartz tube was sealed off without exposure to air and transferred to the spectrometer.

3. Results

3.1. TEMPERATURE PROGRAMMED REDUCTION

Fig. 1 shows the reduction profiles of 3% Pd/KL after calcination up to different temperatures, T_c. For $T_c = 250°C$ there is a single hydrogen consumption peak at 150°C; the peak area suggests a hydrogen consumption exceeding one hydrogen molecule for every Pd ion as expected if all the ions were in the Pd^{2+} oxidation state. After calcination up to 350°C, there are three hydrogen consumption peaks at 0, 70 and 150°C. Contrary to the catalysts calcined at

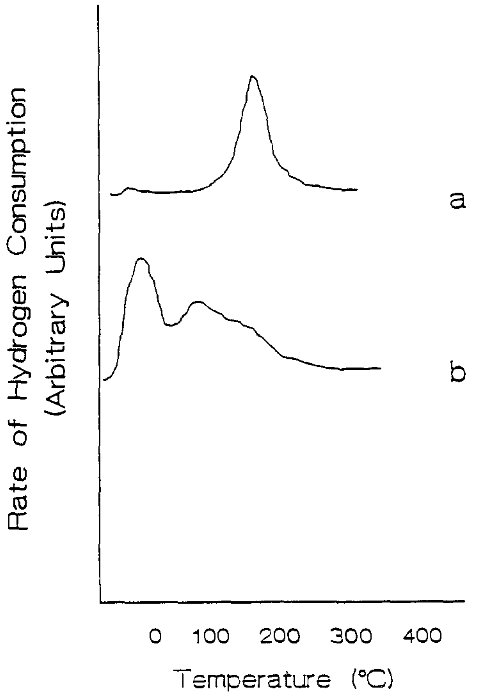

Fig. 1. TPR spectra for Pd/KL after calcination up to (a) 250°C and (b) 350°C.

250°C, the hydrogen consumption in this case is lower than the expected value of 1 H_2/Pd. In table 1, the hydrogen consumption during TPR is represented as the change in valence of Pd (ΔV_1), which is calculated as

$$\Delta V_1 = (2 \times \text{moles of } H_2 \text{ consumed})/\text{moles Pd}.$$

3.2. TEMPERATURE PROGRAMMED REDUCTION-MASS SPECTROMETRY

Figs. 2 and 3 show the mass spectra observed during temperature programmed reduction of Pd/KL after calcination up to 250 and 350°C, respectively. After calcination up to 250°C, we see a similar hydrogen consumption profile at 150°C, with evolution of ammonia at 500°C. After calcination up to

Table 1
Hydrogen consumption represented as $\Delta V = H/Pd$ for first TPR (ΔV_1) and second TPR after reoxidation (ΔV_2)

Catalyst	T_c	ΔV_1	ΔV_2
3% Pd/KL	250	2.7	2.1
	350	1.5	2.0
	400	1.4	2.1

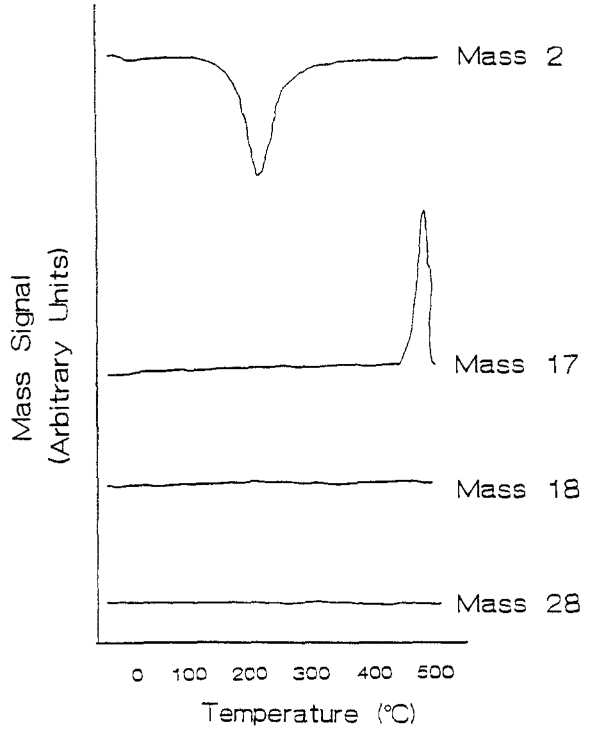

Fig. 2. TPR-MS spectra for Pd/KL after calcination up to 250°C.

350°C, we see a hydrogen consumption profile similar to that which is observed with the TCD cell. However, we do not see any evolution of water, ammonia or nitrogen which implies that the hydrogen consumption is due to the reduction of Pd ions.

3.3. TPR-REOXIDATION

After reoxidation at 100°C, we expect all the Pd to be present in the form of PdO. Reduction of this product in the second TPR should give us a hydrogen consumption of 1 H_2/Pd. Fig. 4 shows the second TPR profile for Pd/KL (IE) which had previously been calcined up to 350°C. A single low temperature peak at 0°C is observed which is probably due to reduction of PdO. The hydrogen consumption is indeed equal to $H_2/Pd = 1$ (see table 1) i.e. $\Delta V_2 = 2$. This result which was confirmed for a sample previously calcined up to 250°C, shows that the ΔV values obtained from TPR integration are correct and reliable. The values $\neq 2$ in the first TPR are therefore not experimental artifacts, but indicate real deviations from the simple chemistry of reduction of Pd^{2+} ions to Pd^0 atoms.

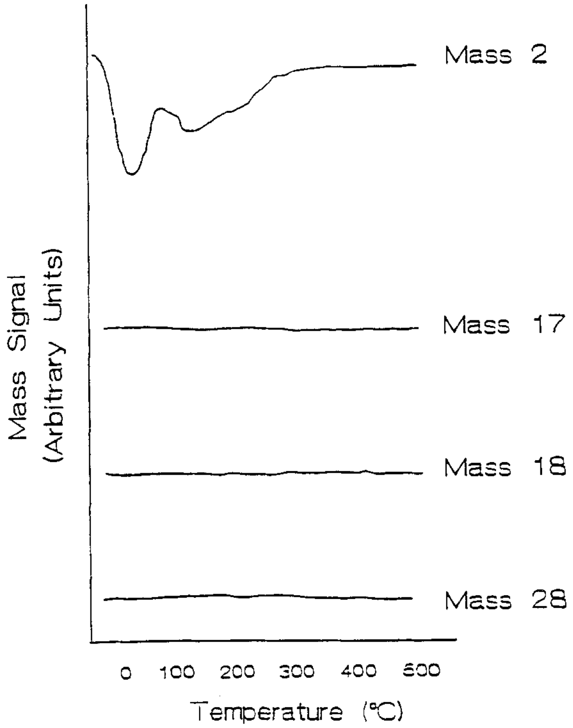

Fig. 3. TPR-MS spectra for Pd/KL after calcination up to 350°C.

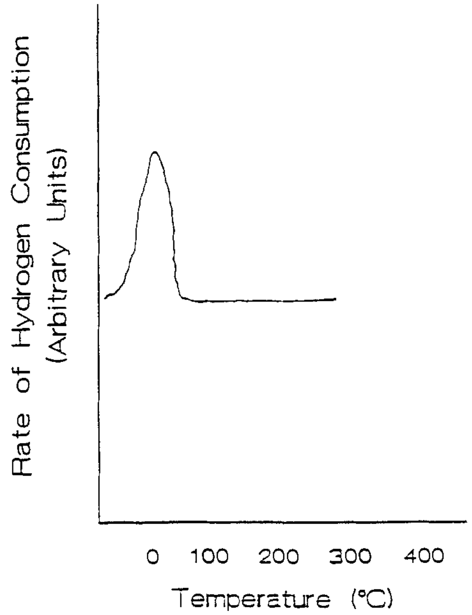

Fig. 4. TPR spectra after reoxidation at 100°C for 1 h, after initial calcination up to 350°C and first TPR up to 300°C.

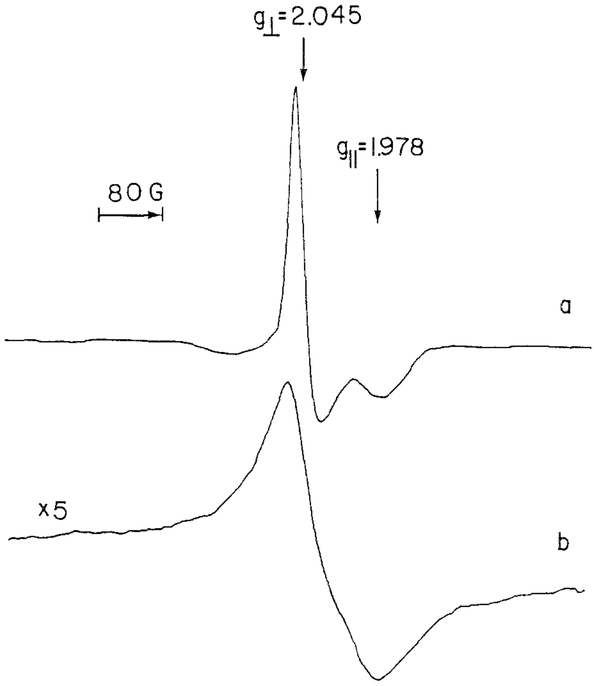

Fig. 5. EPR spectra at room temperature for Pd/KL (a) calcined up to 350°C, and (b) calcined up to 350°C and exposed to 10 Torr of O_2.

3.4. ELECTRON PARAMAGNETIC RESONANCE SPECTROSCOPY (EPR)

Fig. 5 shows the EPR spectrum at room temperature for Pd/KL (IE) which was calcined up to 350°C. The spectrum shows a strong EPR signal with $g_\parallel = 1.978$ and $g_\perp = 2.045$ which indicates the presence of a paramagnetic Pd species having an axial symmetry. By comparison with a $CuSO_4 \cdot 5H_2O$ standard, approximately 3% of Pd are paramagnetic after calcination up to 350°C. Further calcination up to 500°C does not change the EPR signal. Also included in fig. 5 is the spectrum recorded at room temperature of 3% Pd/KL calcined up to 350°C and exposed to 10 Torr of O_2. In this case we observe that the EPR signal broadens out significantly due to the dipolar interaction with O_2. At 77 K, the spectrum for this sample changes back to the original spectrum obtained after calcination up to 350°C.

These results prove that after calcination some of the Pd ions are present in an oxidation state $\neq 2$.

4. Discussion

The hydrogen consumption values calculated from the TPR experiments for 3 wt% Pd/KL show that after calcination up to 350°C, the ΔV values are lower than 2, but after calcination up to 250°C, the ΔV values are higher than 2. This implies that either some of the Pd is not in the form of Pd^{2+} or there is some error in measurement using the TCD cell. These two possibilities will be discussed in turn.

If we have some ammonia left over in the catalyst after calcination and the cold trap at the exit of the reactor is not efficient in removing it, then ammonia can pass through the sample side of the TCD cell either as ammonia or its decomposition products and interfere with the TCD measurements. Since ammonia has a thermal conductivity similar to argon, this would dilute the exit stream in hydrogen and lead to an apparent ΔV higher than 2. To further investigate these possibilities, we look to the results of the TPR-MS experiments. The absence of the cold trap at the outlet of the reactor enables us to monitor all the products of the reduction. The TPR-MS spectra in fig. 2 for Pd/KL (IE) after calcination up to 250°C indicate that the ammine ligands do not leave the catalyst during hydrogen reduction until the temperature is increased beyond 450°C.

Fig. 3 shows that during TPR after calcination up to 350°C, no products of reduction leave the catalyst. The electron paramagnetic resonance studies indicate that a paramagnetic Pd species is present in the ion-exchanged catalysts after calcination up to 350°C. Among the possible oxidation states of Pd, only Pd^{1+} (d^9) and Pd^{3+} (d^7) are paramagnetic with $s = 1/2$. Pd^{1+} and Pd^{3+} in zeolites have been reported by Michalik et al. [18,19] and Ghosh and Kevan [20]. The presence of Pd^{1+} is excluded in our case since the signal remains unchanged after further calcination up to 500°C. Pd^{3+} ions have been known to form after calcination up to 500°C in X and Y zeolites [18–20]. Thus we conclude that the EPR signal is due to part of the Pd ions being in the form of Pd^{3+}.

This species has an axial g tensor with $g_{\perp} > g_{\parallel} > g_e$. A tetragonally elongated octahedron with a $d_{z^2-r^2}$ ground state will result in such a g value [24].

In zeolite KL, only the cation sites in the cancrinite cage (site B) and the hexagonal prism (site A) [25] can have an octahedral geometry. Pd^{3+} in the hexagonal prism has been reported to give an isotropic EPR signal [20] which is not affected by O_2 absorption. The strong dipolar broadening observed upon O_2 absorption suggests that this species is located in the cancrinite cage (site B), since it is more accessible to O_2.

Thus the Pd^{3+} species must be in the cancrinite cage where it experiences a distorted octahedral field and results in an axial EPR signal. Since the TPR gives us low ΔV values and there is no EPR signal for the reduced sample, it follows that after reduction the Pd^{3+} ions in the cancrinite cage are only partially reduced, presumably to Pd^{2+}.

We also separately studied Pd catalysts supported on L zeolite which was previously modified by exchanging the K^+ ions for Ca^{2+} ions and driving these Ca^{2+} ions into the cancrinite cages by calcination [26]. In this case the Ca^{2+} ions in the cancrinite cages are expected to prevent the migration of Pd ions to the cancrinite cage. As expected, the relative EPR intensity of this sample is approximately 60% weaker than that of the Pd/KL sample, further supporting the claim that the Pd^{3+} ions are located in the cancrinite cage.

However, after reoxidation with O_2 all the Pd is present as PdO, and in the subsequent TPR it is reduced with $H_2/Pd = 1$ or ΔV_2 of 2. This might indicate that in an O_2 atmosphere, the Pd ions migrate from the cancrinite cages to the main channel, where Pd^{2+} is more stable than Pd^{3+}. From the TPR spectra in figs. 1 and 4 we see that both PdO and Pd^{2+} ions are reduced at 0°C and cannot be differentiated on the basis of the TPR peak position alone. After the second TPR all the Pd is present in the form of Pd^0 and resides in the main channel.

Since Pd is easily oxidized to Pd^{3+} during calcination whereas ammine ligands decompose only at 300°C under O_2 environment, it is possible that Pd^{3+} exists in the main channel as an ammine complex after calcination up to 250°C. During reduction all the Pd is reduced, and this would lead to a ΔV value higher than 2 due to the reduction of Pd^{2+} and Pd^{3+} in the main channel.

5. Conclusions

The results indicate that Pd^{3+} is formed, besides Pd^{2+}, during calcination of $Pd(NH_3)_4^{2+}$ in zeolite L. The Pd^{3+} ions are detected by their EPR signal. After calcination below 300°C, these ions are in the main channel, presumably as ammine complexes. Their reduction leads to hydrogen consumption with $H_2/Pd > 2$. At higher calcination temperatures, Pd^{3+} ions are located in the cancrinite cage, where they are only reduced to Pd^{2+}. In an oxygen atmosphere, Pd ions return to the main channel and are present as PdO and Pd^{2+}.

Acknowledgement

Financial support by the National Science Foundation, Contract No. CTS-8911184/02, is gratefully acknowledged.

References

[1] J.R. Bernard, *Proc. 5th Int. Conf. on Zeolites* (Heyden, London, 1980) p. 66.

[2] C. Besoukhanova, J. Guidot, D. Barthomeuf, D. Breysse and J.R. Bernard, J. Chem. Soc. Faraday Trans. 77 (1981) 1595.

[3] G. Larsen and G.L. Haller, Catal. Lett. 3 (1989) 103.

[4] S.J. Tauster and J.J. Steger, J. Catal. 125 (1990) 387.

[5] S.J. Tauster and J.J. Steger, Mat. Res. Soc. Symp. Proc. 111 (1988) 419.

[6] W.E. Alvarez and D.E. Resasco, Catal. Lett. 8 (1991) 53.

[7] D.J. Ostgard, L. Kustov, K.R. Poeppelmeier and W.M.H. Sachtler, J. Catal. 133 (1992) 342.

[8] E.G. Derouane and D.J. Vanderveken, Appl. Catal. 45 (1988) L15.

[9] E.G. Derouane, J.B. Nagy, C. Fernandez, Z. Gabelica, E. Laurent and P. Maljean, Appl. Catal. 40 (1988) L1.

[10] E. Iglesia, J.E. Baumgartner and K.D. Rose, Abstracts of papers of the American Chemical Society, 202 (August) (1991) 15.

[11] H. Lieske, G. Lietz, H. Spindler and J. Völter, J. Catal. 81 (1983) 8.

[12] M. Kraft and H. Spindler, *Proc. 4th Int. Congr. on Catalysis*, Moscow 1968, Vol. 2 (Akad. Kiadó, Budapest, 1971) p. 286.

[13] N.R. Bursian, S.B. Kogan and S.A. Davydova, Kinet. Katal. 9 (1968) 661.

[14] K. Foger and H. Jaeger, Appl. Catal. 56 (1988) 137.

[15] W.J. Reagen, A.W. Chester and G.T. Kerr, J. Catal. 69 (1981) 89.

[16] S.T. Homeyer and W.M.H. Sachtler, J. Catal. 117 (1989) 91.

[17] S.T. Homeyer and W.M.H. Sachtler, J. Catal. 118 (1989) 266.

[18] J. Michalik, M. Narayana and L. Kevan, J. Phys. Chem. 89 (1985) 4553.

[19] J. Michalik, M. Heming and L. Kevan, J. Phys. Chem. 90 (1986).

[20] A.K. Ghosh and L. Kevan, J. Phys. Chem. 94 (1990) 1953.

[21] F. Blatter and K.W. Blazey, J. Phys. Chem. Sol. 52 (1991) 629.

[22] M.S. Tzou, B.K. Teo and W.M.H. Sachtler, J. Catal. 113 (1988) 220.

[23] S.H. Park, M.S. Tzou and W.M.H. Sachtler, Appl. Catal. 24 (1986) 85.

[24] Y. Ben Taârit, J.C. Védrine, J.K. Dutel and C. Naccache, J. Magn. Reson. 31 (1978) 251.

[25] R.M. Barrer and H. Villiger, Z. Krist. 128 (1969) 352.

[26] P.A. Newell and L.V.C. Rees, Zeolites 3 (1983) 22.